Mechanism of Copper Passivation in Aqueous Sodium Carbonate−Bicarbonate Solution Derived from Combined X-ray Photoelectron Spectroscopic and Electrochemical Data

S. González, M. Pérez, M. Barrera, A. R. González Elipe,† and R. M. Souto*

Department of Physical Chemistry, University of La Laguna, E-38205 La Laguna (Tenerife), Spain

Received: February 11, 1998

X-ray photoelectron spectroscopy (XPS) was used to characterize the passivating films anodically formed on copper in $NaHCO_3$ and Na_2CO_3 aqueous solutions (9−11 pH range). The influence of potential and solution pH on the composition and protective characteristics of the passivating layers was considered. The analysis of the experimental data supports the composed nature of the formed films. Direct evidence regarding the addition of carbonate species to the surface layers in potential ranges positive to the onset of Cu(II) oxides formation was achieved from XPS data. Specific components of the XPS signals attributable to carbonate species present in the passivating films could be identified.

1. Introduction

The passive films formed on the surface play an important role in corrosion stability of copper, thus the passivation and corrosion of copper in neutral and alkaline aqueous electrolytes has been the subject of numerous electrochemical investigations.[1−23] Oxidation and reduction processes result in a series of surface oxides which may eventually incorporate secondary corrosion products. It is well established that the passive films formed on copper in oxygen-free NaOH solutions consist of Cu_2O and CuO or $Cu(OH)_2$ depending on the electrode potential.[4] The relative amount of material related to these layers depends on pH, potential, anodization time, and temperature.[10−16] The employment of diverse electrochemical techniques to study the behavior of copper in different aqueous media has demonstrated that considerable dissolution of the metal takes place even in a passive state.[11,13]

Various spectroscopic methods have also been used for the study of the structure and the identification of the oxidizing states participating in the passivating films on copper, namely, ion-scattering spectroscopy (ISS),[4] X-ray photoelectron spectroscopy (XPS),[4,19,25−27] ellipsometry,[28,29] photoacustic spectroscopy,[30] Raman spectroscopy,[31] extended X-ray absorption fine structure spectroscopy (EXAFS),[32] grazing incidence X-ray diffractometry (GIXD), and Fourier transform infrared (FTIR) spectroscopies.[33] From these studies it has been concluded that $Cu(OH)_2$ is present in the copper(II) potential regime. Accordingly, copper oxide films may show a single or a duplex structure depending on the applied electrode potential.

The breakdown of passive films is determined by the loss of pH control at the surface due to proton generation,[21] thus resulting in enhanced metal dissolution. Furthermore, the formation of passivating films as well as metal dissolution of copper in alkaline solutions can be strongly influenced by the nature of anions present in the solution.[15−17,20,22] Most anions may favor a more extensive attack of the metal, eventually leading to pitting corrosion.[11,16,17,23,24] Nevertheless, it has been observed that in aqueous solutions containing either carbonate[17,22,34] or phosphate[20,35] the protective characteristics of the anodic layers could be improved, though this effect depends considerably on the pH and the relative concentration of anions in the solution. Indeed, it has been observed that carbonate and phosphate ions exert an inhibiting effect on the corrosion of copper as they counter the aggressive attack of pitting-promoting anions such as chloride or sulfate.[36−38]

The electrochemical behavior of copper in carbonate- and bicarbonate-containing aqueous solutions has been the subject of several publications.[17,21,22,34,39] The stability of the passive films formed on copper in these solutions has been found to depend on pH, carbonate−bicarbonate concentration ratio, and hydrodynamics.[22] Thus, the electrochemical behavior of copper has been tentatively explained by considering that the passivating layers formed on the metal are composed layers in which basic copper carbonates precipitate without interfering appreciably with the formation of copper oxides.[17,22] In this way, the initial stages of the passive layer formation should involve the formation of a thin inner Cu_2O layer followed by the growth of a $CuO/Cu(OH)_2-CuCO_3$ complex outer layer. The $Cu(OH)_2$/basic copper carbonates ratio would depend on both the solution pH and the applied potential program. This observation would be in agreement with the thermodynamic observation that for the ternary $Cu-CO_2-H_2O$ system, the precipitation of the species $CuCO_3-Cu(OH)_2$ (malachite) and $2CuCO_3-Cu(OH)_2$ (azurite) is possible.[21,39]

Despite the number of publications about copper corrosion and passivity in carbonate-containing aqueous solutions, the exact composition and structure of the passive films formed on copper from these media has not been established, as SEM and EDAX have been the only nonelectrochemical techniques used so far for the characterization of the system.[17,36] Therefore, it is interesting from both the fundamental and practical standpoint to study the influence of carbonate ions on the composition and structure of the passive films with other techniques sensitive to their chemical nature.

It was the aim of this work to examine the formation and reduction of passivating layers on polycrystalline copper in carbonate-containing aqueous solution at a ionic strength 0.1 M and at different pH ($9 \leq pH \leq 11$). Besides electrochemical studies, XPS measurements were performed to determine the chemical nature of these layers. Results from electrochemical measurements are briefly presented and discussed in relation to the XPS findings.

† Institute of Materials Science, CSIC, Seville, Spain.
* Corresponding author.

S1089-5647(98)01069-4 CCC: $15.00
Published on Web 06/20/1998

2. Experimental Section

Working electrodes (specimens) were made from electrolytic copper rods of 99.9% purity. Drawn copper rods 0.8 cm in diameter were machined to obtain cylindrical specimens 0.3 cm in diameter. The base of the copper cylinder was used as a horizontal disk working electrode in contact with a hanging electrolyte solution column.[40] The specimens were thermally treated at 500 °C under 3 mm Ar gas pressure for 2 h, to eliminate residual mechanical stresses and to improve their surface homogeneity. Then each specimen was electropolished in 85% H_3PO_4 (by weight),[20] rinsed with twice distilled water, and, finally, dried in air at room temperature. This pretreatment assured the reproducibility of results.

The test solution consisted of twice-distilled water to which analytical grade chemicals were added such as Na_2CO_3 and $NaHCO_3$.

Electrochemical measurements were made using a conventional three-electrode Pyrex glass cell containing aqueous 0.1 M Na_2CO_3, pH 11, or 0.1 M $NaHCO_3$, pH 9, at 25 °C, saturated with Ar. The potential of each specimen was measured against a saturated calomel electrode (SCE) provided with a conventional Luggin-Haber capillary tip arrangement. A large cylindrical platinum grid around the specimen was used as the counter electrode. All electrochemical runs were made at 25 °C.

Each electrochemical experience was started with a new copper specimen and a fresh stagnant solution. The working electrode was initially set at $E_{s,c} = -1.00$ V for 3 min to ensure a completely electroreduced copper surface. Single (STPS) and repetitive triangular potential sweeps (RTPS) were applied to the specimen at a scan rate of 0.01 V s^{-1}.

XPS spectra of copper specimens were obtained with an electron spectrometer ESCALAB 210 (Vacuum Generator Ltd., U.K.). Procedures of reduction, passivation, and passive film breakdown on the copper surface in the carbonate solution were similar to those for the electrochemical measurements. The electrodes were taken out of the solution at a given potential, rinsed with twice distilled water, and then dried under argon flow. Once introduced in the spectrometer, specimens were irradiated with Al Kα radiation with a mean energy of 1486.6 eV. The specimen container was evacuated to 5×10^{-7} Torr and held at 308 K. The photoelectron spectra corresponding to O 1s, C 1s, Cu 2p and Cu-AES signals were measured. The binding energies at the peaks observed in the photoelectron spectra were corrected by using the value of the energy of the C 1s level observed at the background spectrum.

3. Results

3.1. Voltammetric Characterization. Voltammetric techniques were used to establish the potential ranges of the different electrochemical reactions occurring during the electrochemical oxidation of copper specimens and subsequent electroreduction in carbonate-containing aqueous solution. The voltammograms of copper recorded at a sweep rate of 0.01 V s^{-1} in 0.1 M Na_2CO_3 (pH 11) and in 0.1 M $NaHCO_3$ (pH 9) solutions at room temperature are plotted in Figures 1 and 2, respectively. Potential limits were defined between −1.00 V(SCE) and a positive potential sufficiently high to include either oxygen evolution or passive film breakdown. Before running the voltammograms a prepolarization of 3 min at the cathodic limit was imposed with the objective of reducing surface oxides.

From the inspection of Figure 1, measured in 0.1 M Na_2CO_3 solution, two well-defined anodic peaks (A_I and A_{II}) related to the formation of Cu_2O and $CuO/Cu(OH)_2$ can be observed at −0.34 and −0.08 V(SCE), respectively. Above 0.0 V(SCE),

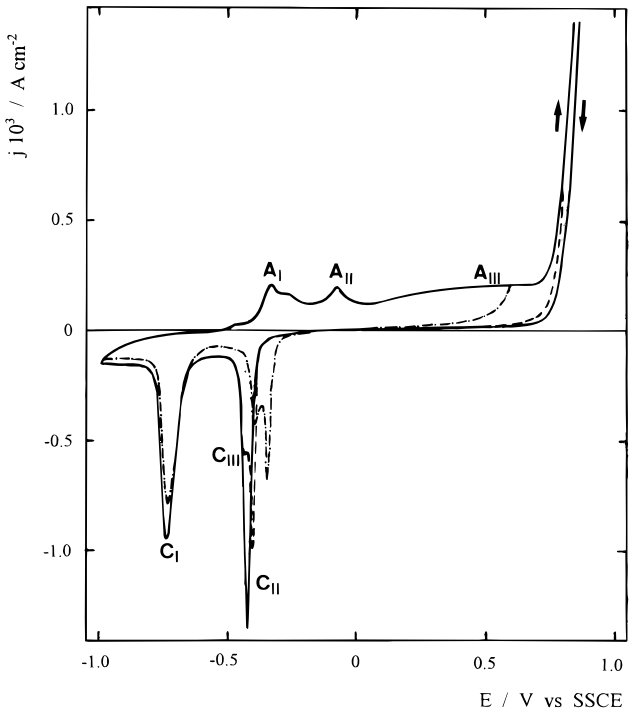

Figure 1. Voltammograms run for copper electrodes in 0.1 M Na_2CO_3 solution at 0.01 V s^{-1}; 25 °C. The voltammetric sweep commences at −1.0 V. The influence of $E_{s,a}$ can be observed in three consecutive runs.

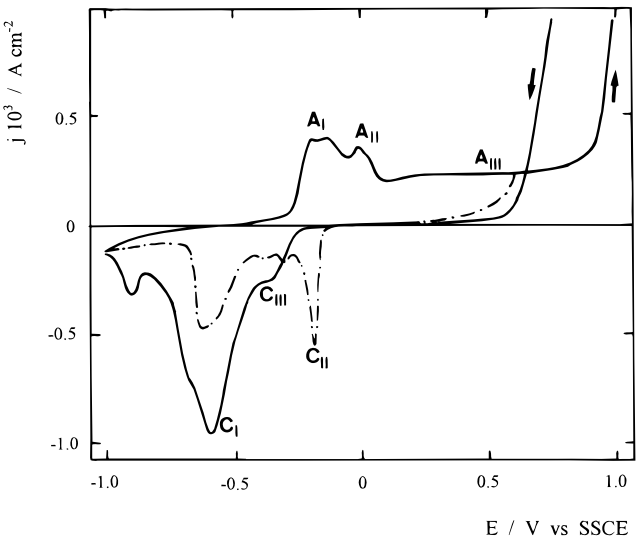

Figure 2. Voltammograms run for copper electrodes in 0.1 M $NaHCO_3$ solution at 0.01 V s^{-1}; 25 °C. The voltammetric sweep commences at −1.0 V. The influence of $E_{s,a}$ can be observed in two consecutive runs.

an anodic current plateau (A_{III}) extending up to 0.72 V(SCE) is found. Further excursion of the potential to more positive values results in an abrupt increase of the current flowing in the system, which indicates that the oxygen evolution reaction (OER) commences. The reverse potential scan shows three cathodic peaks (C_I, C_{II}, and C_{III}). The potential values at which these electroreduction peaks are observed depend on the extent of the previous anodic sweep. This effect is especially noticeable for peaks C_{II} and C_{III} and reflects aging effects in the film derived from the different anodization time applied in each run. Reduction peaks C_{II} and C_I can be assigned to the electroreduction of $CuO-Cu(OH)_2$ to Cu_2O, and Cu_2O to Cu, respectively, analogously to the reduction processes occurring in plain NaOH solutions.[12] However, peak C_{III}, which has only been

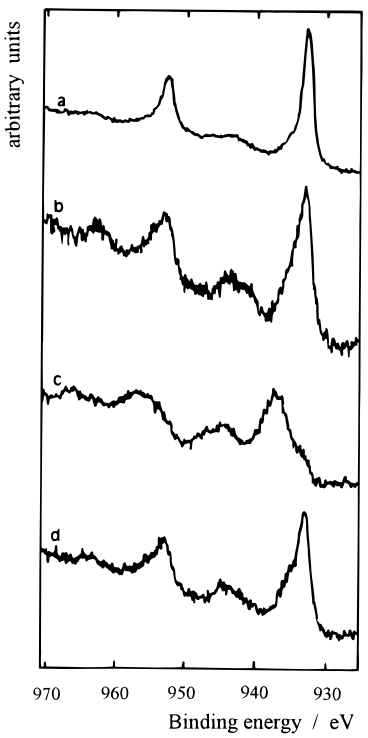

Figure 3. XPS spectra in Cu 2p region from copper specimens anodized at 0.01 V s^{-1} in 0.1 M Na_2CO_3 solution. $E_{s,c} = -0.80$ V(SCE). Specimens were taken at potential values (a) −0.34 V, (b) 0.65 V, (c) 1.0 V, and (d) −0.50 V during the negative-going scan; the preceding positive-going scan was extended up to $E_{s,a} = 0.65$ V(SCE).

observed in carbonate-containing aqueous solutions,[22] should be associated with the electroreduction of a Cu carbonate−Cu hydroxide layer formed at potentials more positive than 0.0 V(SCE).

Analogously, voltammograms were also recorded for a new copper specimen immersed in 0.1 M $NaHCO_3$ solution, as depicted in Figure 2, and are for the most part qualitatively analogous to those depicted in Figure 1, though the potentials of the voltammetric peaks are shifted with pH.[22] It should be noted that the extent of the stability potential range for the anodic films produced on copper is smaller in this case, as passive film breakdown is encountered at potential values of ca. 0.80 V(SCE). However, as the applied potential exceeds ca. 0.80 V(SCE), a rapid anodic increase is observed, whereas the reverse scan shows a remarkable counterclockwise hysteresis loop, which indicates that the critical breakdown potential of passivated copper in the solution has been exceeded. The repassivation potential is observed at the potential value for which the current trace intersects that obtained during the positive-going scan (at ca. 0.60 V(SCE)). Thus, decrease of pH promotes the localized attack of copper in the potential region where the OER takes place, as observed by SEM.[22]

Therefore, from an electrochemical point of view, regarding the state of the passive films existing on the copper surface, four different situations could be generally observed. During the positive-going scan, first the copper(I) potential regime is entered, as only a Cu_2O film is expected at potentials up to that of peak A_I (case a). Next the copper(II) potential regime is encountered; that is, further excursion of potential into the positive direction leads to the growth of the passive film eventually through the formation of a CuO−Cu carbonate complex outer layer, which comprises the potential range of peak A_{II} and the passive regime A_{III} (case b). When the potential for the oxygen evolution reaction is passed during the positive-going polarization, high currents are driven through the system, which might result in modifications of the passive film (case c). Finally, partial electroreduction of the passive film is achieved at potentials covered by peaks C_{II} and C_{III}, though a passivating layer (case d) is still present on the electrode surface at −0.50 V. Complete electroreduction of the surface layers is only achieved when the electroreduction process responsible for peak C_I is performed. These four cases are observed in the carbonate-containing solution bearing the higher pH value under study (for copper in 0.1 M Na_2CO_3, pH 11), but case c could not be considered in the solution with the lower pH because localized breakdown of the passive film occurs at potential values negative to those where the OER occurs.

3.2. XPS Data. XPS analysis has been used to determine the valence states of copper at the surface of copper electrodes after electrochemical polarization in order to understand the effect of carbonate ions.

For the chemical identification of the copper surface species, analysis of both Cu 2p and Cu LMM Auger lines was performed.[41,42] The presence of Cu^{2+} in CuO is characterized by high-intensity shake-up satellites which appear at ca. 10 eV higher binding energy than the main $2p_{3/2}$ and $2p_{1/2}$ lines (933.1, 953.0 eV) and are considerably broader than in the case of bulk Cu_2O and Cu metal.[41−44] It is more difficult to differentiate between copper metal and Cu_2O since the shape and binding energy of the Cu *2p* lines are very similar (931.9, 951.8 eV). However, copper metal and Cu_2O can be distinguished from the X-ray-excited Cu LMM Auger spectra, as the binding energy of the main line increases by 1.6 eV for Cu_2O (568.9 eV) relative to the copper metal (567.3 eV) due to differences in relaxation energies in these materials.

Procedures of oxidation and reduction of the copper surface in the carbonate-ion-containing solution were similar to those for the electrochemical measurements described above. In 0.1 M Na_2CO_3 solution, the electrodes were taken out of the solution at preset potentials in the copper(I), copper(II), and oxygen evolution regimes of the metal, which are labeled as cases a, b, and c, respectively, as well as after partial electroreduction of the passive layers (case d). Then they were rinsed with twice-distilled water and dried under argon atmosphere before measuring the corresponding XPS spectra (Figures 3−6). Specimens were taken at the potential values −0.34, 0.70, and 1.00 V, during the positive-going scan, corresponding to the potential ranges of peak A_I, current plateau A_{III}, and OER, respectively, thus covering cases a−c. Additional specimens were also removed from the solution during the subsequent negative-going potential branch of the voltammogram after partial electroreduction of the passive film formed during the positive-going scan (case d). In this case, $E_{s,a}$ was set at 0.70 V and the specimens were removed from solution at −0.50 V.

For those specimens anodized at potentials lower than the onset of peak A_{II}, XPS data indicate the formation of copper(I) on the surface. No satellite structure can be observed from the Cu 2p spectra as depicted in Figure 3a, thus discarding the formation of higher valence copper species. Furthermore, the corresponding Cu LMM Auger (Figure 4a), O 1s (Figure 5a), and C 1s (Figure 6a) spectra of the same specimen show a very good agreement with the features and energies observed for a Cu_2O film. Higher valences for copper on anodized specimens could only be found from XPS data when the onset potential of voltammetric peak A_{II} was passed during the voltammetric scan.

However, for those specimens anodized at potentials more positive than the onset of peak A_{II}, as well as for those anodized

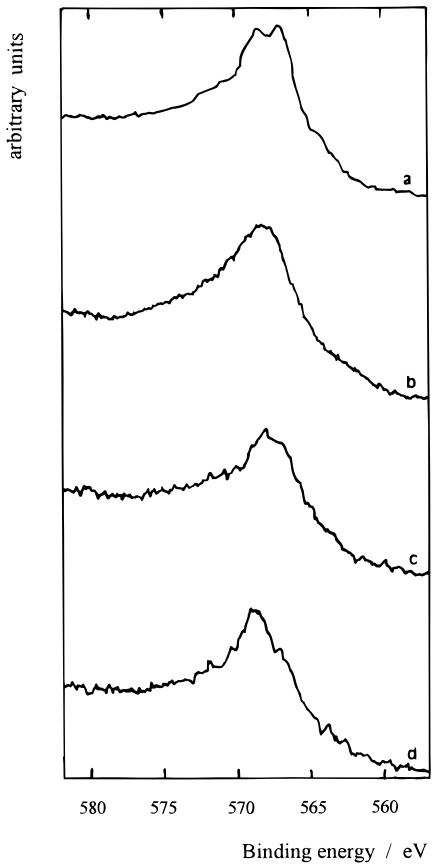

Figure 4. XPS spectra in Cu LMM Auger region from copper specimens anodized at 0.01 V s^{-1} in 0.1 M Na_2CO_3 solution. $E_{s,c} = -0.80$ V(SCE). Specimens were taken at potential values (a) −0.34 V, (b) 0.65 V, (c) 1.0 V, and (d) −0.50 V during the negative-going scan; the preceding positive-going scan was extended up to $E_{s,a} = 0.65$ V(SCE).

in region A_{III}, XPS data revealed the presence of divalent copper at the surface. Shake-up satellites can be observed from the Cu 2p spectra given in Figure 3b, and the features found in the corresponding Cu LMM Auger (Figure 4b), O 1s (Figure 5b), and C 1s (Figure 6b) spectra could agree quite well with those reported for a CuO standard,[39,41] though a certain broadening of the peaks to reach higher binding energies could be observed in all cases. This effect is more significant for the main Cu 2p peaks, which exhibit rather asymmetric shapes.

Modification of the XPS spectra is observed in all cases for those specimens anodized at potentials higher than the onset of the oxygen evolution reaction. In this case, merging of additional contributions occurring at higher binding energies could be clearly observed from the corresponding Cu 2p (Figure 3c), Cu *LMM* Auger (Figure 4c), O 1s (Figure 5c), and C 1s (Figure 6c). Deconvolution of the complex peaks observed in this case still results in the observation of the signals related to the formation of CuO on the surface of the metal, though these signals are mostly covered by the new signals at higher energies. Clear splitting of the two signals is indeed observed in the case of the C 1s spectrum, where a strong signal is observed at higher binding energies than the adventitious C 1s peak at 284.9 eV. Thus, the low binding energy oxygen is probably due to oxygen in the oxide lattice, while the high binding energy oxygen could be due to another oxygen-containing molecule. These observations provide an indication of the presence of copper(II) carbonates at the surface of the specimen.

Partially electroreduced specimens were also observed with the XPS method, as depicted in Figures 3d, 4d, 5d, and 6d. In this case, the measured spectra closely resemble those obtained for the specimens polarized in the copper(II) potential regime

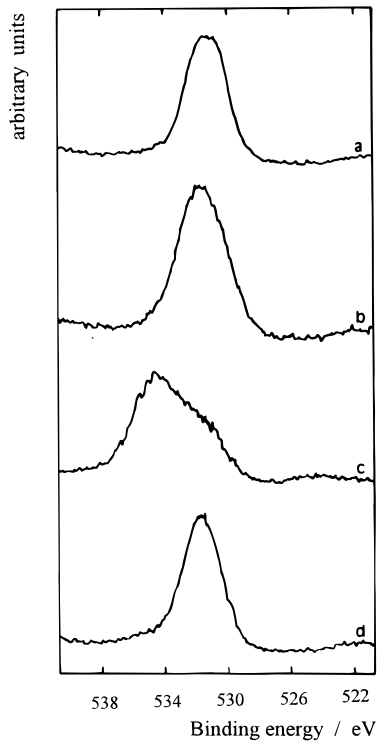

Figure 5. XPS spectra in O 1s region from copper specimens anodized at 0.01 V s^{-1} in 0.1 M Na_2CO_3 solution. $E_{s,c} = -0.80$ V(SCE). Specimens were taken at potential values (a) −0.34 V, (b) 0.65 V, (c) 1.0 V, and (d) −0.50 V during the negative-going scan; the preceding positive-going scan was extended up to $E_{s,a} = 0.65$ V(SCE).

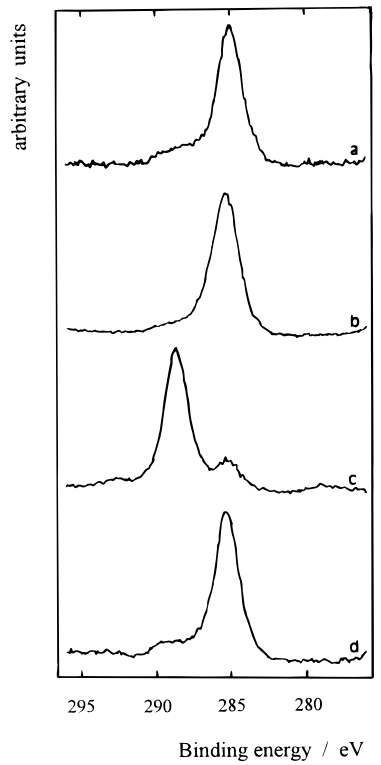

Figure 6. XPS spectra in C 1s region from copper specimens anodized at 0.01 V s^{-1} in 0.1 M Na_2CO_3 solution. $E_{s,c} = -0.80$ V (SCE). Specimens were taken at potential values (a) −0.34 V, (b) 0.65 V, (c) 1.0 V, and (d) −0.50 V during the negative-going scan; the preceding positive-going scan was extended up to $E_{s,a} = 0.65$ V(SCE).

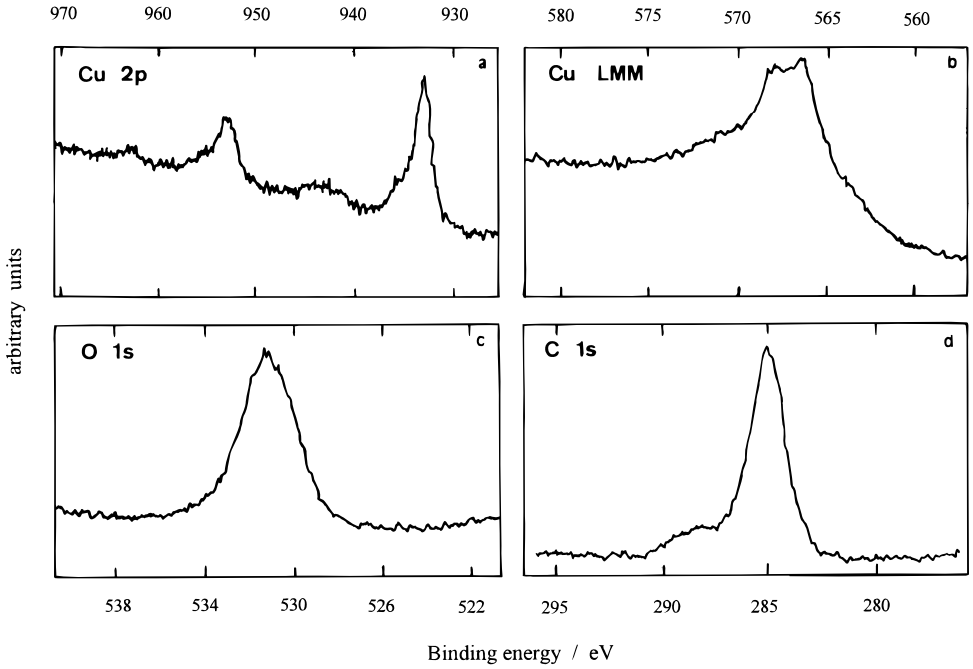

Figure 7. XPS spectra of (a) Cu 2p, (b) Cu LMM Auger, (c) O 1s, and (d) C 1s for the copper specimen anodized at 0.01 V s^{-1} in 0.1 M $NaHCO_3$ solution. $E_{s,c} = -0.80$ V(SCE); $E_{s,a} = 0.60$ V(SCE).

(case b), thus supporting the electrochemical conclusion that the first electroreduction stage involves the reduction of the copper(II)−oxide layer to the univalent state. It must be further noticed the splitting of two signals in the C 1s spectrum (Figure 6d), from which a signal at ca. 290 eV is clearly observed in the partially reduced passive film remaining in the copper surface after the electroreduction processes that take place in the potential range of voltammetric peaks C_{II} and C_{III}.

Finally, XPS spectra were also recorded for specimens polarized in 0.1 M $NaHCO_3$ in the potential ranges of copper(I) and copper(II) oxidation regimes, as well as after partial electroreduction of the passive film (case d). No significant differences could be detected in relation to the corresponding XPS spectra recorded at pH 11 for cases a and d, namely, in the copper(I) regime and after partial electroreduction. Quite significant is the observation of higher bonding energies for all the XPS signals, as well as the splitting of the C 1s signal at more negative potentials than in 0.1 M Na_2CO_3, thus becoming clearly observed in the entire copper(II) potential regime (cf. Figure 7).

4. Discussion

4.1. Preliminary Considerations. X-ray photoelectron spectroscopy is becoming an increasingly used technique for the chemical characterization of electrochemically formed adlayers at electrodes. The ability both to determine elemental composition and to identify specific chemical information in the critical surface region makes this method a particularly useful complement to electrochemical and spectroscopic in situ measurements. The surface chemistry of copper provides an excellent example of this. Nevertheless, it has to be noted that caution should be exercised in the data interpretation because the method necessitates the removal of the electrode from the electrochemical cell for observation under high vacuum, as destruction or modification of the surface layer during the transfer cannot be completely discarded.

Experiments described in this work correspond to the electrochemical behavior of copper in aqueous carbonate-ion-containing solutions at pH 11 and 9. Despite the presence of adventitious carbon in the specimens, our results have shown that the anodic layers formed in these media contain carbon, which is consistent with the formation of an insoluble copper carbonate-containing layer during copper anodization.

The global reactions that can be involved in copper anodization in carbonate-containing solutions can be summarized as follows:

$$2Cu + H_2O = Cu_2O + 2H^+ + 2e^- \qquad E^\circ = 0.229 - 0.059\ \text{pH} \quad (1)$$

$$Cu_2O + H_2O = CuO + 2H^+ + 2e^- \qquad E^\circ = 0.427 - 0.059\ \text{pH} \quad (2)$$

$$Cu + H_2O = CuO + 2H^+ + 2e^- \qquad E^\circ = 0.328 - 0.059\ \text{pH} \quad (3)$$

$$Cu^+ + OH^- = CuOH \qquad pK_s = 14.7 \quad (4)$$

$$Cu^{2+} + 2OH^- = Cu(OH)_2 \qquad pK_s = 19.9 \quad (5)$$

$$Cu^{2+} + CO_3^{2-} = CuCO_3 \qquad pK_s = 9.63 \quad (6)$$

$$Cu^{2+} + 2OH^- + CO_3^{2-} + 2Na^+ = Cu(OH)_2(CO_3)Na_2 \qquad pK_s = 15.0 \quad (7)$$

$$2Cu^{2+} + 2OH^- + CO_3^{2-} = Cu(CO_3)\cdot Cu(OH)_2\ \text{(malachite)} \qquad pK_s = 33.78 \quad (8)$$

$$3Cu^{2+} + 2OH^- + 2\,CO_3^{2-} = 2Cu(CO_3)\cdot Cu(OH)_2\ \text{(azurite)} \qquad pK_s = 45.96 \quad (9)$$

where either the corresponding standard equilibrium potential (E°) or pK_s value at 25 °C is indicated as taken from the

literature.[47,48] In addition, the following ionic equilibria in solution were also considered in the pH range covered in this work:

$$H_2CO_3 = H^+ + HCO_3^- \qquad pK_{a1} = 6.35 \qquad (10a)$$

$$HCO_3^- = H^+ + CO_3^{2-} \qquad pK_{a2} = 10.33 \qquad (10b)$$

Therefore, in the $9 \leq pH \leq 11$ range, thermodynamic data support that the anodic layers formed on copper in carbonate-containing solution involve three main constituents, namely, copper(II)−oxide, copper(I)−oxide, and copper(II)−basic carbonates. This assumption implies a nonhomogeneous passive layer, as supported by those results depicted in Figure 1, which shows the occurrence of three different processes from the voltammograms, in the potential range of peaks A_I and A_{II} and in the current plateau A_{III}. On the other hand, the overall anodic oxide layer electroreduction takes place in two well defined potential ranges, namely, in the −0.25 to −0.50 V range and in the −0.60 to −0.80 V. The electrochemical processes occurring at voltammetric peaks C_{II} and C_{III} are related to the electroreduction to copper(I) of the copper(II) species present on the surface.

4.2. Interpretation of XPS Data. The interpretation of XPS spectra of Cu specimens after electrochemical treatments in aqueous carbonate solutions has been based on the variations observed on Cu 2p, Cu-AES, O 1s, and C 1s signals from the specimens anodized at different potentials. The analysis of the data showed that an oxide film had formed on the surface, and eventually carbonate incorporation could be observed as well depending on the potential achieved during the anodization process.

Copper was present in both univalent and divalent states, indicating the presence of Cu_2O and CuO, though the presence of copper(II) basic carbonates had to be considered in order to explain the XPS spectra measured for specimens anodized in the copper(II) potential regime. The observed formation of these oxides and basic carbonates correlates well with thermodynamics since the free energy at room temperature associated with the oxidation reactions is always a negative value.

The combination of the experimental data supports the composed nature of the formed films, which comprise an inner Cu_2O and an outer $CuO/Cu(OH)_2-CuCO_3$ complex layer. Copper carbonates precipitate as long as soluble ionic copper species are produced, without interfering appreciably with the formation of copper oxides. The relative amount of material related to these layers depends on solution pH and applied potential, becoming more noticeable as the potential is set more positive at a given pH, or at lower pH values for a given applied potential value.

Additional research is planned in our group in an attempt to get more information regarding the (possible) interactions existing between the oxide duplex layer responsible for copper passivity and the copper carbonates precipitated on it. In this case, the in situ application of some other spectroelectrochemical tehcniques is being considered, which should provide additional information regarding the structure of the anodic films grown from copper in carbonate-containing aqueous solutions.

5. Conclusions

We have by using the surface-sensitive XPS technique examined the composition and chemical state of the passive layers formed on copper specimens after electrochemical oxidation and reduction cycles in carbonate-containing aqueous solutions in the $9 \leq pH \leq 11$ range. XPS analysis of copper after electrochemical treatments in these solutions showed that an oxide film had formed on the surface, and eventually carbonate incorporation could be observed as well. In this case, polarization of the copper specimens in the copper(II) potential regime was necessary. These results support much of our previous work concerning the electrochemical behavior of copper in carbonate-containing aqueous solutions,[17,39] with enhanced corrosion resistance due to the formation of copper basic carbonates.

The anodic layer formed on copper anodized in carbonate-containing solution was found to contain copper in both univalent and divalent oxidation states and to display specific XPS signals attributable to carbonate species present in the electrode surface films. This result agrees with the electrochemical observations consistent with the addition of copper carbonate species in the passive film developed on copper without appreciably interfering with the structure of the duplex oxide layer responsible for copper passivity which is spontaneously formed in alkaline aqueous media.

Acknowledgment. This work was supported by the Gobierno de España (Dirección General de Enseñanza Superior) under Grant 96/1031.

References and Notes

(1) Ambrose, J.; Barradas, R. G.; Shoesmith, D. W. *J. Electroanal. Chem.* **1973**, *47*, 47.
(2) Ambrose, J.; Barradas, R. G.; Shoesmith, D. W. *J. Electroanal. Chem.* **1973**, *47*, 65.
(3) Shoesmith, D. W.; Rummery, T. E.; Owen, D.; Lee, W. *J. Electrochem. Soc.* **1976**, *123*, 790.
(4) Strehblow, H. H.; Titze, B. *Electrochim. Acta* **1980**, *25*, 839.
(5) Droog, J. M. M.; Alderliesten, C. A.; Alderliesten, P. T.; Bootsma, G. A. *J. Electroanal. Chem.* **1980**, *111*, 61.
(6) Droog, J. M.; Schlenter, B. *J. Electroanal. Chem.* **1980**, *112*, 387.
(7) Shoesmith, D. W.; Sunder, S.; Bailey, M. G.; Wallace, G. J.; Stanchell, F. W. *J. Electroanal. Chem.* **1983**, *143*, 153.
(8) Strehblow, H. H.; Speckmann, H. D. *Werkst. Korros.* **1984**, *35*, 512.
(9) de Chialvo, M. R. G.; Marchiano, S. L.; Arvia, A. J. *J. Appl. Electrochem.* **1984**, *14*, 165.
(10) Speckmann, H. D.; Lohrengel, M. M.; Schultze, J. W.; Strehblow, H. H. *Ber. Bunsen-Ges. Phys. Chem.* **1985**, *89*, 392.
(11) de Chialvo, M. R. G.; Salvarezza, R. C.; Vásquez Moll, D. V.; Arvia, A. J. *Electrochim. Acta* **1985**, *30*, 1501.
(12) de Chialvo, M. R. G.; Zerbino, J. O.; Marchiano, S. L.; Arvia, A. J. *J. Appl. Electrochem.* **1986**, *16*, 517.
(13) Gómez Becerra, J.; Salvarezza, R. C.; Arvia, A. J. *Electrochim. Acta* **1988**, *33*, 613.
(14) Wanner, M.; Wiese, H.; Weil, K. G. *Ber. Bunsen-Ges. Phys. Chem.* **1988**, *92*, 736.
(15) Elsner, C. I.; Salvarezza, R. C.; Arvia, A. J. *Electrochim. Acta* **1988**, *33*, 1735.
(16) Drogowska, M.; Brossard, L.; Ménard, H. *Surf. Coat. Technol.* **1988**, *34*, 383.
(17) Pérez Sánchez, M.; Barrera, M.; González, S.; Souto, R. M.; Salvarezza, R. C.; Arvia, A. J. *Electrochim. Acta* **1990**, *35*, 1337.
(18) Nishikata, A.; Itagaki, M.; Tsuru, T.; Haruyama, S. *Corros. Sci.* **1990**, *31*, 287.
(19) Collisi, U.; Strehblow, H.-H. *J. Electroanal. Chem.* **1990**, *284*, 385.
(20) Laz, M. M.; Souto, R. M.; González, S.; Salvarezza, R. C.; Arvia, A. J. *Electrochim. Acta* **1992**, *37*, 655.
(21) Tromans, D.; Sun, R.-H. *J. Electrochem. Soc.* **1992**, *139*, 1945.
(22) Pérez Sánchez, M.; Souto, R. M.; Barrera, M.; González, S.; Salvarezza, R. C.; Arvia, A. J. *Electrochim. Acta* **1993**, *38*, 703.
(23) Souto, R. M.; Pérez Sánchez, M.; Barrera, M.; González, S.; Salvarezza, R. C.; Arvia, A. J. *Electrochim. Acta* **1992**, *37*, 1437.
(24) Souto, R. M.; González, S.; Salvarezza, R. C.; Arvia, A. J. *Electrochim. Acta* **1994**, *39*, 2619.
(25) McIntyre, N. S.; Sunder, S.; Shoesmith, D. W.; Stanchell, F. W. *J. Vac. Sci. Technol.* **1981**, *18*, 714.
(26) Shoesmith; D. W.; Sunder, S.; Bailey, M. G.; Wallace, G. J.; Stanchell, F. W. *J. Electroanal. Chem.* **1983**, *143*, 153.
(27) Kautek, W.; Gordon, J. G. *J. Electrochem. Soc.* **1990**, *137*, 2672.

(28) Yamashita, M.; Omura, K.; Hirayama, D. *Surf. Sci*. **1980**, *96*, 443.
(29) Ord, J. L.; DeSmet, D. J.; Huang, Z. Q. *J. Electrochem. Soc*. **1987**, *134*, 826.
(30) Sander, U.; Strehblow, H. H.; Dohrmann, J. K. *J. Phys. Chem.* **1981**, *85*, 447.
(31) Hamilton, J. C.; Farmer, J. C.; Anderson, R. J. *J. Electrochem. Soc*. **1986**, *133*, 739.
(32) Strehblow, H.-H.; Borthen, P.; Druska, P. *Synchrotron Techniques in Interfacial Electrochemistry;* Melendres, C. A., Tadjeddine, A., Eds.; Kluwer Academic: Dordrecht, 1994; p 295.
(33) Kautek, W.; Geuss, M.; Sahre, M.; Zhao, P.; Mirwald, S. *Surf. Coat. Technol*. **1997**, *25*, 548.
(34) Ribotta, S. B.; Folquer, M. E.; Vilche, J. R. *Corrosion (NACE)* **1995**, *51*, 682.
(35) Souto, R. M.; Laz, M. M.; González, S. *An. Quim. Int. Ed*. **1997**, *93*, 252.
(36) Drogowska, M.; Brossard, L.; Ménard, H. *J. Electrochem. Soc*. **1992**, *139*, 39.
(37) Milosev, I.; Metikos-Hukovic, M.; Drogowska, M.; Ménard, H.; Brossard, L. *J. Electrochem. Soc.* **1992**, *139*, 2409.
(38) Drogowska, M.; Brossard, L.; Ménard, H. *J. Appl. Electrochem*. **1994**, *24*, 344.
(39) van Muylder, J. *Comprehensive Treatise of Electrochemistry;* Bockris, J. O'M., Conway, B. E., Yeager, E., White, R. E., Eds.; Plenum Press: New York, 1981; Vol. 4, p 1.
(40) Elsner, C. I.; Shilardi, P.; Marchiano, S. L. *J. Appl. Electrochem*. **1993**, *23*, 1181.
(41) Souto, R. M.; Fox, V.; Laz, M. M.; Pérez, M.; González, S. *J. Electroanal. Chem*. **1996**, *411*, 161.
(42) Souto, R. M.; Laz, M. M.; González, S. *J. Phys. Chem. B* **1997**, *101*, 508.
(43) Kim, K. S. *J. Electron. Spectrosc. Relat. Phenom.* **1974**, *3*, 217.
(44) Benndorf, C.; Caus, H.; Egert, B.; Seidel, H.; Theime, F. *J. Electron. Spectrosc. Relat. Phenom.* **1980**, *19*, 77.
(45) Fleisch, T. H.; Mains, G. K. *Appl. Surf. Sci*. **1982**, *10*, 51.
(46) Tobin, J. P.; Hirshwald, W.; Cunningham, J. *Appl. Surf. Sci*. **1983**, *16*, 441.
(47) Pourbaix, M. *Atlas of Electrochemical Equilibria in Aqueous Solutions*; Pergamon Press: London, 1965.
(48) Smith, R. M.; Martell, A. E. *Critical Stability Constants*; Pergamon Press: New York, 1976; Vol. 4.